(Received 10 May 2025, Accepted 1 July 2025, Scheduled 19 July 2025)

Dipole Antenna with U and L-Shaped Stubs on Multiple I-Shaped EBG for Digital Television Applications

Natchayathorn Wattikornsirikul[1], Suwat Sakulchat[2,*], Watcharaphon Naktong[3,*], and Sommart Promput[4]

[1]*Department of Aircraft Maintenance Engineering, Faculty of Railway Systems and Transportation Rajamangala University of Technology Isan, Muang, Nakhon Ratchasima 30000, Thailand*
[2]*Department of Electrical Engineering, Faculty of Engineering and Architecture Rajamangala University of Technology Suvarnabhumi, Phranakhon Si Ayutthaya 13000, Thailand*
[3]*Department of Telecommunication Engineering and Digital Innovation, Faculty of Engineering and Technology Rajamangala University of Technology Isan, Nakhon Ratchasima 30000, Thailand*
[4]*Department of Mechatronics and Robotics Engineering, School of Engineering and Innovation Rajamangala University of Technology Tawan-ok, Chonburi 20110, Thailand*

ABSTRACT: This article presents a dipole antenna with added U- and L-shaped stubs designed with copper plates to support frequencies according to the Digital Video Broadcasting (DVB) standard in the 510–790 MHz range. The dipole antenna was placed on a polyester mylar film substrate with a thickness of 0.3 mm and a dielectric constant of 3.2. The CST program was used for simulating the optimization parameters with a size of $270 \times 15.5 \times 0.59\,\text{mm}^3$ for the use with a flat-screen television. This research uses the technique of reducing signal wave reflection with a 1×41 units I-shaped electromagnetic band gap (EBG) strip, which is made from copper plates, placed beneath the antenna with foam sheets as an intermediary. The distance between the EBG plate and the antenna is appropriately 2 mm, with an impedance bandwidth of 46.01% (502–802 MHz) and a unidirectional pattern, resulting in an average gain of 3.62 dBi. For applications with television structures, installing the antenna and EBG plate at the top position can cover the most suitable frequency range, which is 44.32% (504–791 MHz).

1. INTRODUCTION

Currently, the population in Asia, especially in Thailand, still prefers to consume news or dramas through television and Digital Television (DTV) boxes, which have become indispensable in daily life. The main device for receiving signals is antenna, which is mostly designed with different gains and sizes for various applications [1–5]. The choice of antenna for use depends on the distance from the transmission station. However, the problem encountered when using the antenna is that signal cables must be installed, which may require unnecessary drilling into the existing wall structure. Additionally, when a television is purchased, an extra antenna must always be bought, as many television brands do not come with a DTV antenna installed; they only include an antenna for receiving Wi-Fi signals [6–8]. Based on the aforementioned problem, the authors are interested in developing an antenna for use according to the DVB standard, which can be installed or attached to the television structure. This combines integration with an Electromagnetic Band Gap (EBG) to help reduce the reflection distance of metal from the television and the television's electronic circuit board. In the past, several research groups have focused on antenna design using various techniques that can serve as guidelines for developing DVB antennas as follows.

An I-shaped monopole antenna used a rectangular slotting technique on both sides of the antenna to enable dual-polarization reception of DTV frequency signals. The antenna operated in the frequency range of 470–960 MHz, covering DTV, WiMAX, CDMA/GSM, and E-GSM900 standards. It was used in conjunction with a 3×11 unit rectangular EBG sheet placed 4 mm away from the antenna, with an average gain of 5 dBi [9]. A microstrip antenna used slotted lotus-shaped technique on the radiator to enable the antenna to operate in the frequency range of 7.80–15 GHz according to ultra-wideband (UWB) standard. It was used in conjunction with an 8×6 unit square EBG sheet placed at a distance of 0.5 mm from the antenna, with an average gain of 5 dBi [10]. The electrically small filtenna-based dipole antenna used an S-shaped folding technique on both sides of the antenna, combined with a hybrid ring-filter, to enable the antenna to operate in the frequency range of 1.957–2.093 GHz. It was used in conjunction with an 8×8 unit square EBG sheet with a circular base of 22.56 mm radius, placed at a distance of 10.508 mm from the antenna, achieving an average gain of 5 dBi [11]. The dipole antenna was used for radio frequency identification (RFID) tags and operated at a frequency of 920 MHz and combined with an EBG sheet H-shaped with 4×1 units and an I-shaped in a horizontal axis with 1×5 units, placed at a distance of 2 mm from the antenna. It had a gain of 1.23 dBi with an omnidirectional radiation pattern [12].

* Corresponding authors: Suwat Sakulchat (suwat.sa@rmutsb.ac.th); Watcharaphon Naktong (Watcharaphon.na@rmuti.ac.th).

A circular microstrip antenna used a technique of adding a square stub to the antenna to enable it to operate over a wide band of 3.5–12.4 GHz according to UWB standards. It was used to measure the wave energy in the human body, in conjunction with a 7×7 unit square EBG sheet placed at a distance of 7.9 mm from the antenna, with an average gain of 9.1 dBi [13]. An F-shaped monopole antenna was arranged in a 2×4 unit for smartphone structures. The antenna operated in the frequency range of 3.4–3.8 GHz in a multiple-input multiple-output (MIMO) system and was used in conjunction with a rectangular EBG sheet of 15×8 units placed at a distance of 0.97 mm from the antenna, with an average gain of 5 dBi [14]. A dipole antenna was used for RFID Tags in the frequency range of 0.85–0.95 GHz, in conjunction with a 7×7 unit square EBG plate that had a high impedance surface, placed at a distance of 4.8 mm from the antenna, with an average gain of 5 dBi [15]. A monopole antenna with U-shaped notches was arranged in a 13×4 unit, which had dual-band frequency ranges of 2.5–2.7 GHz and 3.4–3.6 GHz in a MIMO system. The antenna was used in conjunction with a rectangular EBG plate of 7×14 units placed at a distance of 11 mm from the antenna, with gain values ranging from 6.9–7.8 dBi and 7.8–8.6 dBi, respectively [16]. A triangular microstrip antenna with an I-shaped slot had a frequency range of 2.36–2.40 GHz for measuring wave energy in the human body. It was used in conjunction with a 2×2 unit square EBG sheet placed at a distance of 0.97 mm from the antenna, with an average gain of 7.8 dBi [17]. An H-shaped dipole antenna was used for RFID tags in the frequency range of 876–992 MHz, in conjunction with a double-layer symmetric electromagnetic band gap (DLS-EBG) rectangular plate of 2×10 units, placed at a distance of 1.6 mm from the antenna, with an average gain of 1.79 dBi [18]. A square loop antenna was used for RF energy harvesting in the 868 MHz frequency, in conjunction with a 3×3 unit square artificial magnetic conductor (AMC) placed at a distance of 42.3 mm from the antenna. It had an average gain of 7.52 dBi and could harvest a voltage of 1.4 V [19].

An antenna with an inversely E-shaped antenna (IESA) was used to measure the wave energy in the human body in the 2.4 GHz frequency. It was used in conjunction with a square EBG sheet that had a T-shaped stub arranged in a 2×2 unit, placed at a distance of 0.7 mm from the antenna, with an average gain of 7.8 dBi [20]. A triangular microstrip antenna operated in the 2.4 GHz and 5.2 GHz frequency in Wi-Fi systems, in conjunction with a triangular EBG plate consisting of 3×3 units, placed at a distance of 1.4 mm from the antenna, with an average gain of 13 dBi [21]. A dual-polarized 4×4 dipole antenna operated in the frequency range of 1.7–2.2 GHz in Wi-Fi and long term evolution (LTE) systems, in conjunction with a triangular EBG plate of 4×4 units, placed at a distance of 35 mm from the antenna [22]. An E-shaped dipole antenna with 4×4 units operated in the frequency range of 4.48–7.12 GHz in a MIMO system, along with a square EBG plate fabricated of a rhomboid artificial magnetic conductor (AMC) 5×5 units, placed at a distance of 3 mm from the antenna, with an average gain of 8.4 dBi [23]. A 2×2 surface-mount dipole antenna array operated in the frequency range of 24.7–29.9 GHz in a 5G system, covering frequency bands N257 (26.5–29.5 GHz), N258 (24.25–27.5 GHz), and N261 (27.5–28.35 GHz). It was used in conjunction with a circular EBG plate, solder balls, and a solder resist plate with 14×12 units, arranged at a distance of 1.4 mm from the antenna, with an average gain of 9.5 dBi [24]. An I-shaped rectangular microstrip antenna was used to measure the specific absorption rate (SAR) of the human body at a frequency of 2.33 GHz, in conjunction with a circular EBG plate of 2×2 units placed at a distance of 0.787 mm from the antenna [25]. A dipole antenna with a U-shaped stub arranged in a 1×2 configuration was used to measure the SAR in the human body within the frequency range of 2.42–2.70 GHz, in conjunction with an EBG sheet in an I-shape of 11×3 units placed at a distance of 3.2 mm from the antenna [26]. A dipole antenna with an added S-shaped stub for mounting on small aircraft operated in the frequency range of 100–600 MHz in the VHF/UHF band, along with a rectangular reflector placed 40 mm away from the antenna, with an average gain of 3.8 dBi [27].

An I-shaped rectangular microstrip antenna was used to measure the SAR of electromagnetic waves in the human body. It operated in the 2.45 GHz frequency range, combined with a mushroom-like EBG sheet consisting of 6×6 units, placed at a distance of 0.17 mm from the antenna, with a gain value of 5.01 dBi [28]. A microstrip antenna with an I-shaped etching on the ground plane was used to measure the SAR of electromagnetic waves in the human body. It operated in the frequency range of 4.8–7 GHz in conjunction with an 8×8 unit mushroom-shaped polarization conversion electromagnetic band-gap (CPC EBG) placed 2 mm away from the antenna, with a gain of 10.5 dBi [29]. An I-shaped dipole antenna was used in the frequency range of 470–862 MHz in a DTV system, along with a mushroom-like EBG 3×3 units placed at a distance of 60 mm from the antenna, with an average gain of 8.44 dBi [30]. A dipole antenna operated in the frequency range of 2.6 GHz and 3.5 GHz and was used in a WiMAX system in conjunction with mushroom-like EBG 4×6 units. An EBG employed a technique of adding a 1×3 rectangular patch array placed at a distance of 1.27 mm from the antenna, achieving gain values of 4.91 dBi and 4.94 dBi [31]. A dipole antenna was arranged in a crossed dipole with an added circular stub, combined with closed-loop and open-loop plate enhancement techniques, to enable the antenna to receive circularly polarized (CP) signals. It operated in the frequency range of 4.75–5.94 GHz for WLANs and GPS systems, along with a triangular EBG metasurface reflector plate with 4×4 units placed at a distance of 2.1 mm from the antenna, achieving a gain of 6.5–7.7 dBi [32]. A rectangular microstrip antenna in the 2.45 GHz frequency range, combined with mushroom-like EBG 3×3 units and a slot-shaped metamaterial 2×5 units, increased the gain. Placed at a distance of 10 mm from the antenna, with an average gain of 11.97 dBi, it could harvest a voltage of up to 2.82 mV [33].

From the problem mentioned earlier, researchers had the idea to solve the issue by using an antenna instead of a signal cable. This involves designing a dipole antenna with an antenna structure combined with an EBG plate, following the researchers' approach [12, 15], which was developed and tuned together with the stub-adding technique [23, 26], and an I-shaped EBG strip to help reduce the distance between antennas [12, 26]. The

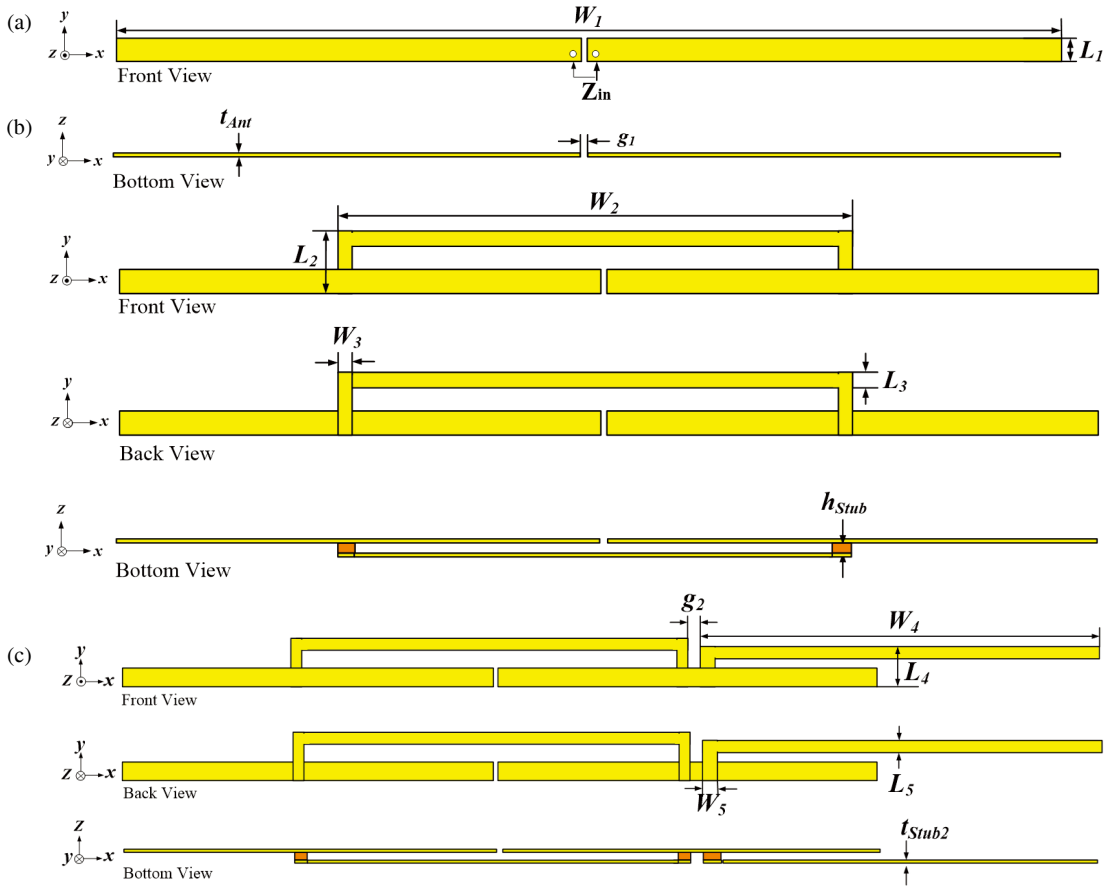

FIGURE 1. Dipole antenna structure (a) in the first step (b) in second step and (c) in third step.

antennas and EBG plates had advantages in terms of easy design and simple structure [28–32] and used low-cost materials, which could help reduce production costs. In the design section, the simulation results of the dipole antenna structure and electromagnetic band gap (EBG) were presented in Section 2. The measurement of antenna properties compared with the simulation results of the reflection coefficient, radiation patterns of E-plane and H-plane, as well as the antenna gain with the electromagnetic bandgap (EBG) are shown in Section 3. The experimental placement of the antenna with the television structure is shown in Section 4. The properties comparison of the proposed antenna with the antennas in previous research is shown in Section 5, and Section 6 summarizes the research.

2. DESIGN AND SIMULATION OF ANTENNA STRUCTURE WITH ELECTROMAGNETIC BANG GAP (EBG)

2.1. Dipole Antenna Design

The proposed dipole antenna structure was designed in three steps. The first step was to design the basic dipole antenna structure using a copper sheet with conductivity (σ) of 5.8×10^7 S/m and a thickness (t_{Ant}) of 0.297 mm. The design was selected at a resonance frequency of 650 MHz to cover the operational frequency range of 510–790 MHz, allowing for the calculation of the antenna width (W_1 equal to 230.75 mm), antenna length (L_1 equal to 5.16 mm), and the distance between antennas (g_1 equals 1.43 mm) as shown in Equations (1)–(3) [2, 34, 35]. Then, the calculated values were simulated using the Computer Simulation Technology (CST) program, as shown in Figure 1(a). Simulating the reflection coefficient (S_{11}), it was found that the basic dipole antenna structure designed in the first step had an impedance bandwidth of 17.40% (600–715 MHz), as shown in Figure 2. The bandwidth obtained did not yet cover the entire frequency range of 510–790 MHz, so the antenna structure needs to be improved to cover the lower frequency range of 500–700 MHz and the higher frequency range of 700–800 MHz.

$$W_1 = \frac{0.5c}{f_r} \tag{1}$$

$$L_1 = \frac{0.02c}{f_r\sqrt{3.2}} \tag{2}$$

$$g_1 = \frac{0.031c}{f_r} \tag{3}$$

The second step in designing the antenna structure was to increase the bandwidth to cover the operating frequency range of 700–800 MHz. The researchers studied the technique of extending the operational frequency range by adding a U-shaped stub, as shown in Figure 1(b). The U-shaped stub structure used

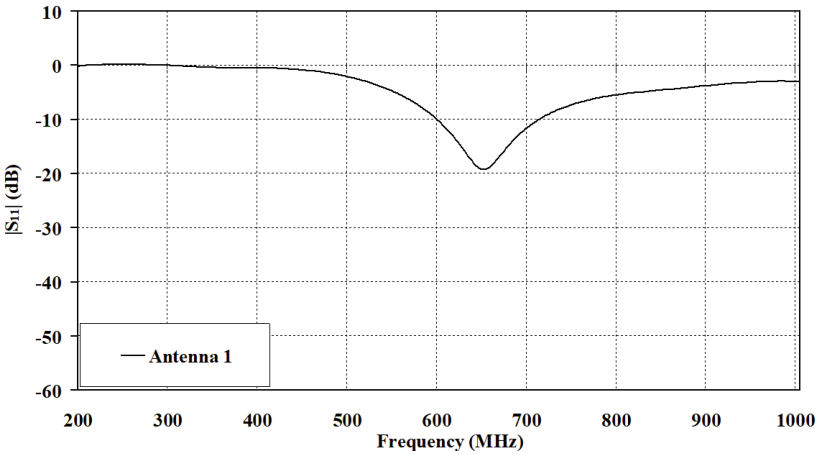

FIGURE 2. Simulation result of reflection coefficient (S_{11}) in the first step.

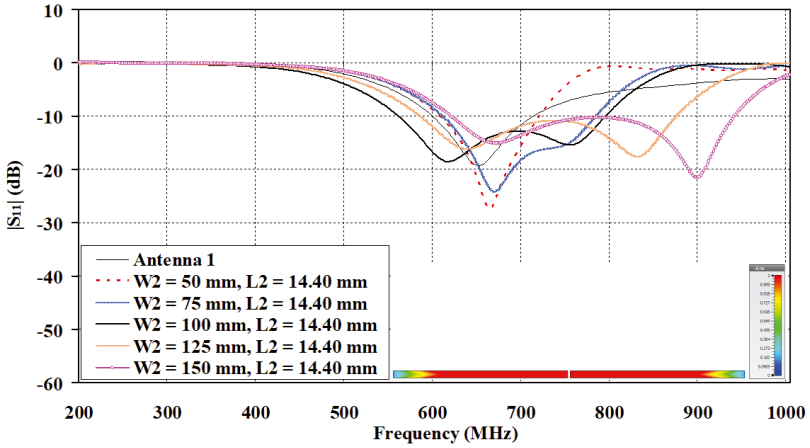

FIGURE 3. Simulation result of S_{11} in the second step, when adjusted W_2.

copper plates, similar to the antenna, and adds a polyester mylar film substrate with a dielectric constant (ε_r) of 3.2 and a thickness (h_{Stub}) of 0.3 mm. The study would be conducted using the technique of adding stub from research [2, 26] in conjunction with the simulation of current density in the antenna. Therefore, we chose to design at a resonance frequency of 750 MHz to cover a wider range of high-frequency operating frequencies. Calculating the width of the body part of the U-shaped stub uses Equation (4) (W_2 equals 100 mm). The length of the arm part of the U-shaped stub could be calculated using Equation (5) (L_2 equals 14.40 mm), and the width of the arm and the length of the body of the U-shaped stub could be calculated using Equation (6) (W_3 and L_3 equal 1.50 mm). By adjusting the parameter width of W_2 from the wavelength value ($0.125\lambda < W_2 < 0.375\lambda$), it could be calculated according to Equation (4), resulting in the range of 50 mm, 75 mm, 100 mm, 125 mm, and 150 mm. The tuning used kept the length L_2 constant, and the optimal width of the U-shaped stub W_2 was 100 mm, with a frequency range of 35.39% (558–798 MHz). This resulted in a wider impedance bandwidth in the higher frequency range as desired, as shown in Figure 3.

$$W_2 = \frac{0.25c}{750 \times 10^6} \tag{4}$$

$$L_2 = \frac{0.036c}{750 \times 10^6} \tag{5}$$

$$W_3 = L_3 = \frac{0.0037c}{750 \times 10^6} \tag{6}$$

In the final step of antenna structure design, the bandwidth must cover the operating low-frequency range of 500–700 MHz. The researchers chose to use L-shaped stub technique [23, 26] as shown in Figure 1(c). The structure of the L-shaped stub used copper sheets as the conductor material, similar to the antenna and substrate material, which was a polyester mylar film, just like the U-shaped stub. Designing the size of the L-shaped stub structure, parameter adjustments will be based on the current density in the antenna.

The resonance frequency of 600 MHz was selected, and calculating the width of the body part of the L-shaped stub was done as per Equation (7) (W_4 equal to 100 mm). The length of the arm part of the L-shaped stub could be calculated as Equation (8) (L_4 equals 7.80 mm). The width of the arm part and the length of the body part of the L-shaped stub could be calculated as Equation (9) (W_5 and L_5 equals 1.95 mm). The width parameter W_4 was adjusted, tuning from the wavelength. It could be calculated as Equation (7), yielding values in the range of

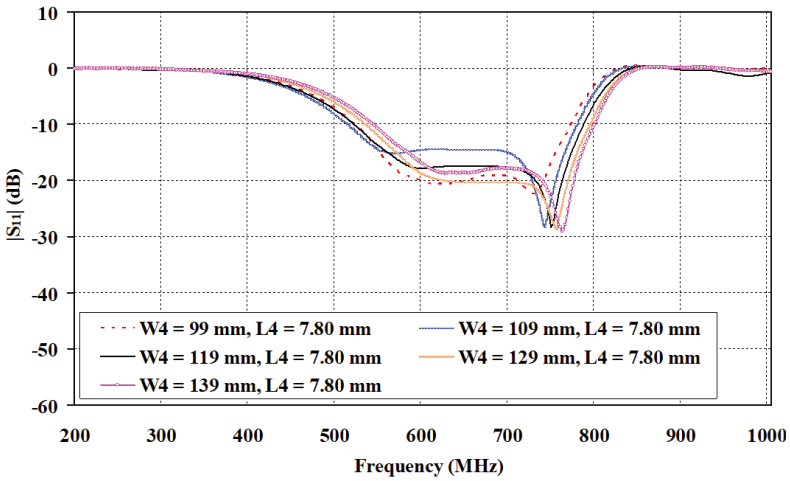

FIGURE 4. Simulation result of S_{11} in the third step, when adjusted W_4.

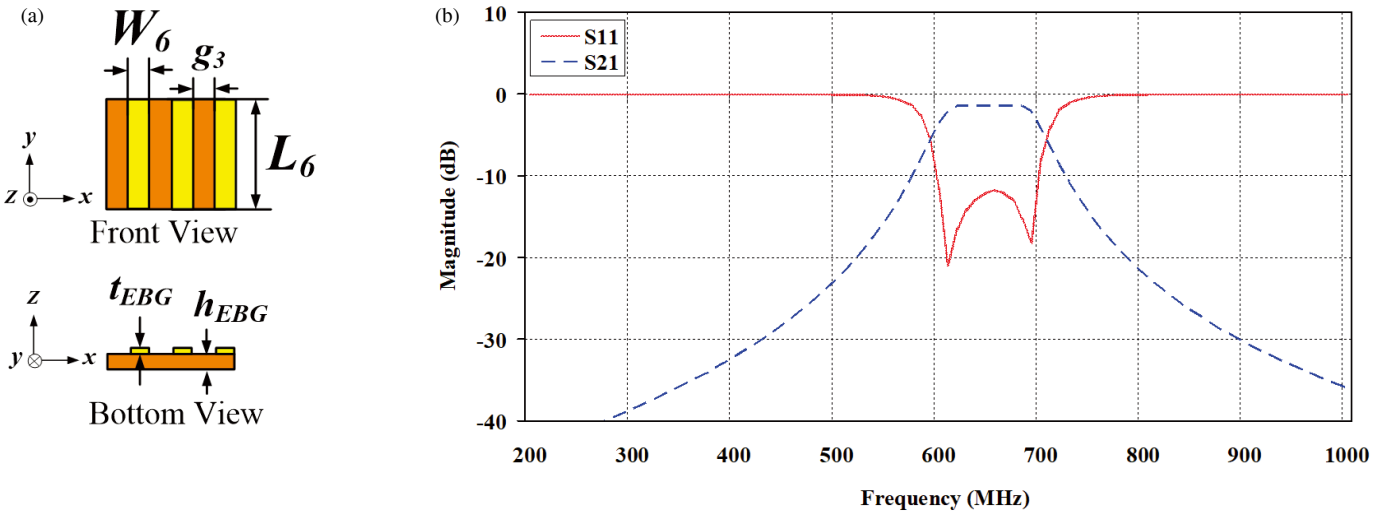

FIGURE 5. Unit cell of I-shaped EBG. (a) structure of arranged I-shaped EBG and (b) simulation result of S_{11} and S_{21} of arranged I-shaped EBG.

99 mm, 109 mm, 119 mm, 129 mm, and 139 mm, while keeping the length of L_4 constant. It was found that the optimal parameter value was W_4 equal to 119 mm, with an operational frequency range of 44.37% (505–793 MHz), covering the desired frequency range of 510–790 MHz, which had an average gain of 1.67 dBi as shown in Figure 4.

$$W_4 = \frac{0.238c}{600 \times 10^6} \tag{7}$$

$$L_4 = \frac{0.0156c}{600 \times 10^6} \tag{8}$$

$$W_5 = L_5 = \frac{0.0039c}{600 \times 10^6} \tag{9}$$

2.2. Design of Electromagnetic Band Gap (EBG)

This section discusses creating a surface to reduce reflections by positioning the antenna in the area above the television. The researcher chose to use an electromagnetic band gap (EBG) with properties of Mu-Epsilon Near Zero (MENZ) [33]. MENZ was a positive value that approached zero. The researchers chose this model for the use with electromagnetic bandgap (EBG) gap plates because MENZ had near-zero properties, which effectively reduced reflection, by choosing copper sheets as the conductor material and polyester mylar film sheets as the substrate material. Design an EBG at a resonance frequency of 650 MHz. The width of the EBG was calculated from Equation (10) (W_6 equals 3.6 mm), and the length of the EBG was calculated from Equation (11) (L_6 equal to 15.5 mm) as shown in Figure 5(a). In terms of the current density flowing through, it influences the inductor (L) of the gap width between the two EGB plates, affecting neighboring patches caused by influencing the inductor (L) of the gap width between the two EGB plates (g_3), affecting neighboring patches caused by the capacitor (C). Additionally, the permeability (μ_o), permittivity (ε_o), and intrinsic impedance (η_o) allow for free space, respectively, by being able to calculate as per Equations (12)–

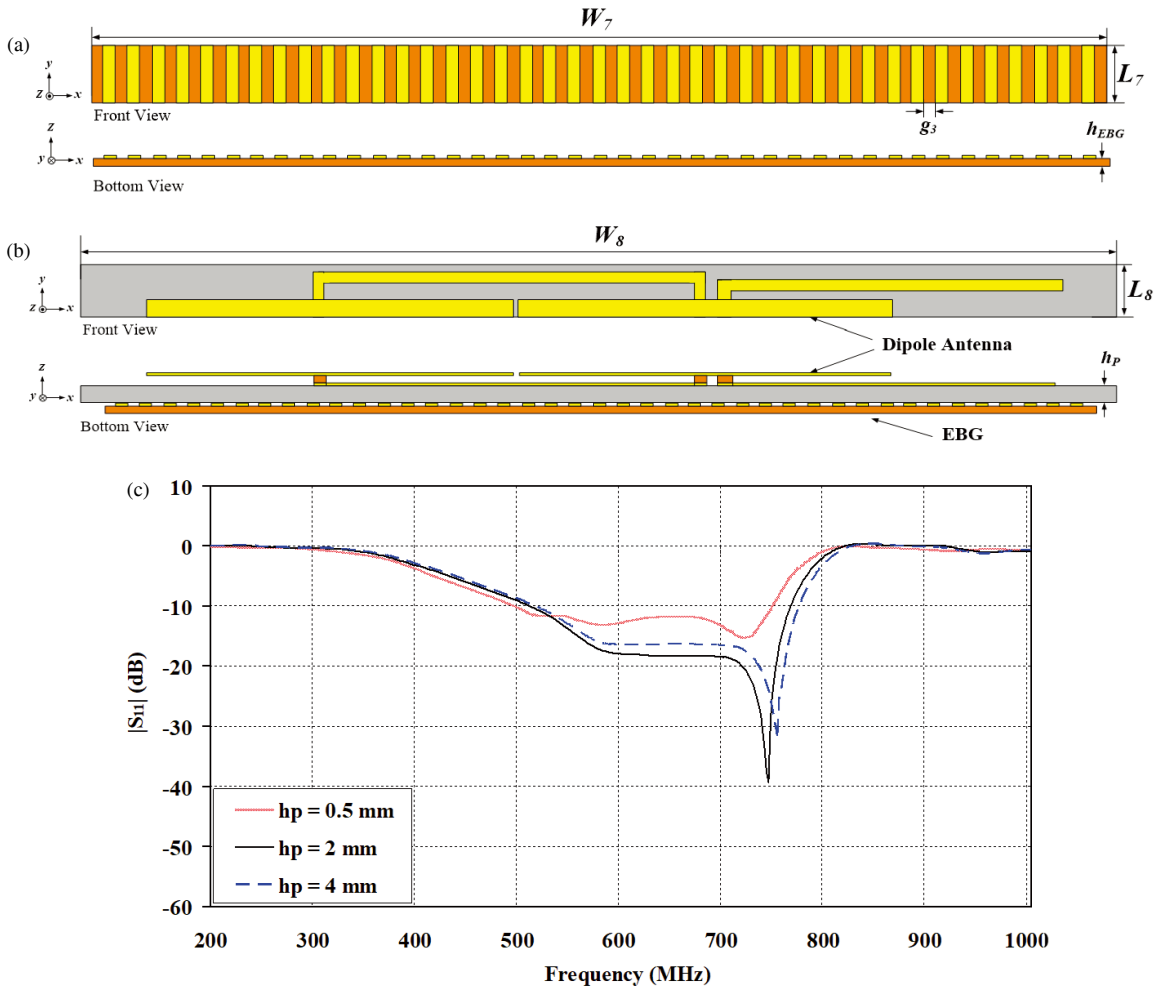

FIGURE 6. Dipole antenna with I-shaped EBG. (a) I-shaped EBG structure (b) dipole antenna with I-shaped EBG on foam sheet and (c) simulation result of S_{11}, when adjusted h_p.

(14) [20, 23]. After that, the obtained values were used to simulate the EBG sheet, and the simulation results showed that the impedance bandwidth covered the frequency range throughout the operating band (600–700 MHz) as shown in Figure 5(b). Next, the EBG plates were arranged along the length of the dipole antenna structure. The EBG plates would be used in a 41×1 unit configuration, with a gap width between the EBG plates (g_3) equal to 3.6 mm, resulting in a total width (W_7) of 270 mm, as shown in Figure 6(a). In terms of placing the antenna on the EGB plate, the distance would be tuned according to the wavelength value ($0.001\lambda < h_p < 0.008\lambda$). The researchers studied techniques from the research in [30–34] to analyze and tune the distance according to the wavelength, using the same distance values for the adjustments, adjusting from 0.5 mm, 2 mm, and 4 mm. The optimal tuning distance was (h_p) equal to 2 mm. The foam sheet was chosen to accommodate the size of the antenna and the EBG sheet appropriately, with a width W_6 of 3.6 mm and a length L_6 of 15.5 mm, as shown in Figure 6(b). The impedance bandwidth had a frequency usage range of 44.01% (505–790 MHz) as shown in Figure 6(c) and an average gain increase of 2.91 dBi with the optimal sizes of various parameters, as shown in Table 1. In the section of the radiation pattern, when simulated by placing the antenna on top of the television, it was found to have a unidirectional pattern in all three frequency bands: 510 MHz, 650 MHz, and 790 MHz as desired, as shown in Figure 7.

$$W_4 = \frac{0.238c}{600 \times 10^6} \tag{10}$$

$$L_4 = \frac{0.0156c}{600 \times 10^6} \tag{11}$$

$$C = \frac{W_6 \varepsilon_o (1+\varepsilon_r)}{\pi} \cosh^{-1}\left(\frac{2W_6 + g_3}{g_3}\right) \tag{12}$$

$$L = \mu_o h_{EBG} \tag{13}$$

$$BW = \frac{1}{\eta_o}\sqrt{\frac{L}{C}} \tag{14}$$

3. ANTENNA PROPERTY MEASUREMENTS

After simulating the antenna structure and obtaining the appropriate parameters, a prototype antenna was fabricated, as shown

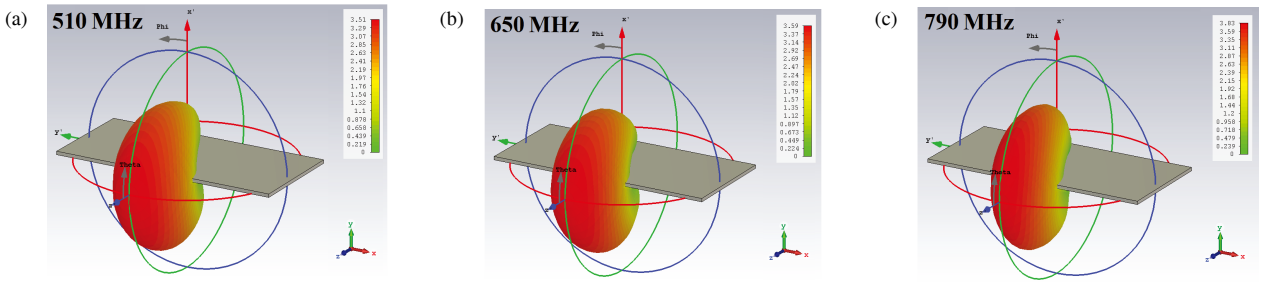

FIGURE 7. Simulation result of radiation pattern (a) at 510 MHz (b) at 650 MHz and (c) at 790 MHz.

TABLE 1. Parameters of rectangular and circular microstrip antennas in the first step.

Parameter	Description	Size (mm)
W_1	The width of dipole antenna	230.75
W_2	The width of body part of U-shape stub	100
W_3	The width of arm part of U-shape stub	1.5
W_4	The width of body part of L-shape	119
W_5	The width of arm part of L-shape	1.95
W_6	The width of I-shape EBG	3.6
W_7	The width of mylar polyester at EBG	270
W_8	The width of foam	270
L_1	The length of dipole antenna	5.768
L_2	The length of arm part of U-shape stub	14.4
L_3	The length of body part of U-shape stub	1.5
L_4	The length of arm part of L-shape	7.80
L_5	The length of body part of L-shape	1.95
L_6	The length of I-shape EBG	15.5
L_7	The length of mylar polyester at EBG	15.5
L_8	The length of foam	15.5
h_{Stub}, h_{EBG}	The thickness of mylar polyester	0.3
h_p	The thickness of foam	2
t_{Ant}, t_{Stub1}, t_{Stub2}, t_{EBG}	The thickness of copper sheet	0.297
g_1	The gap between dipole antenna and ground plane	1.8
g_2	Gap between U-shape stub and L-shape stub	2
g_3	Gap between I-shape EBG and I-shape EBG	3.6

TABLE 2. Comparison properties results of simulation and measurement.

Result	Antenna	BW (%)	Gain (dBi)
Simulation	Dipole	17.40% (600–715 MHz)	1.67
	Dipole with U-shape and L-shape	44.37% (505–793 MHz)	1.89
	Dipole with U-shape and L-shape and with EBG	44.01% (505–790 MHz)	2.91
Measurement	Dipole with U-shape and L-shape	48.72% (503–827 MHz)	1.78
	Dipole with U-shape and L-shape and with EBG	46.01% (502–802 MHz)	2.87

in Figure 8(a). Next, the performance characteristics of the dipole antenna prototype with the E5071C network analyzer will be measured, as shown in Figure 8(b), which measures the reflection coefficient ($S_{11} < -10$ dB) as shown in Figure 8(c). The impedance bandwidth was 46.01% (502–802 MHz), and the average gain was 2.84 dBi, which compared the simulation and measurement results as shown in Table 2. The prepared antenna for measurement of the radiation pattern, as shown in Figure 8(d), was unidirectional, and compared with the simulation results, as shown in Figures 9–10, respectively, it was found

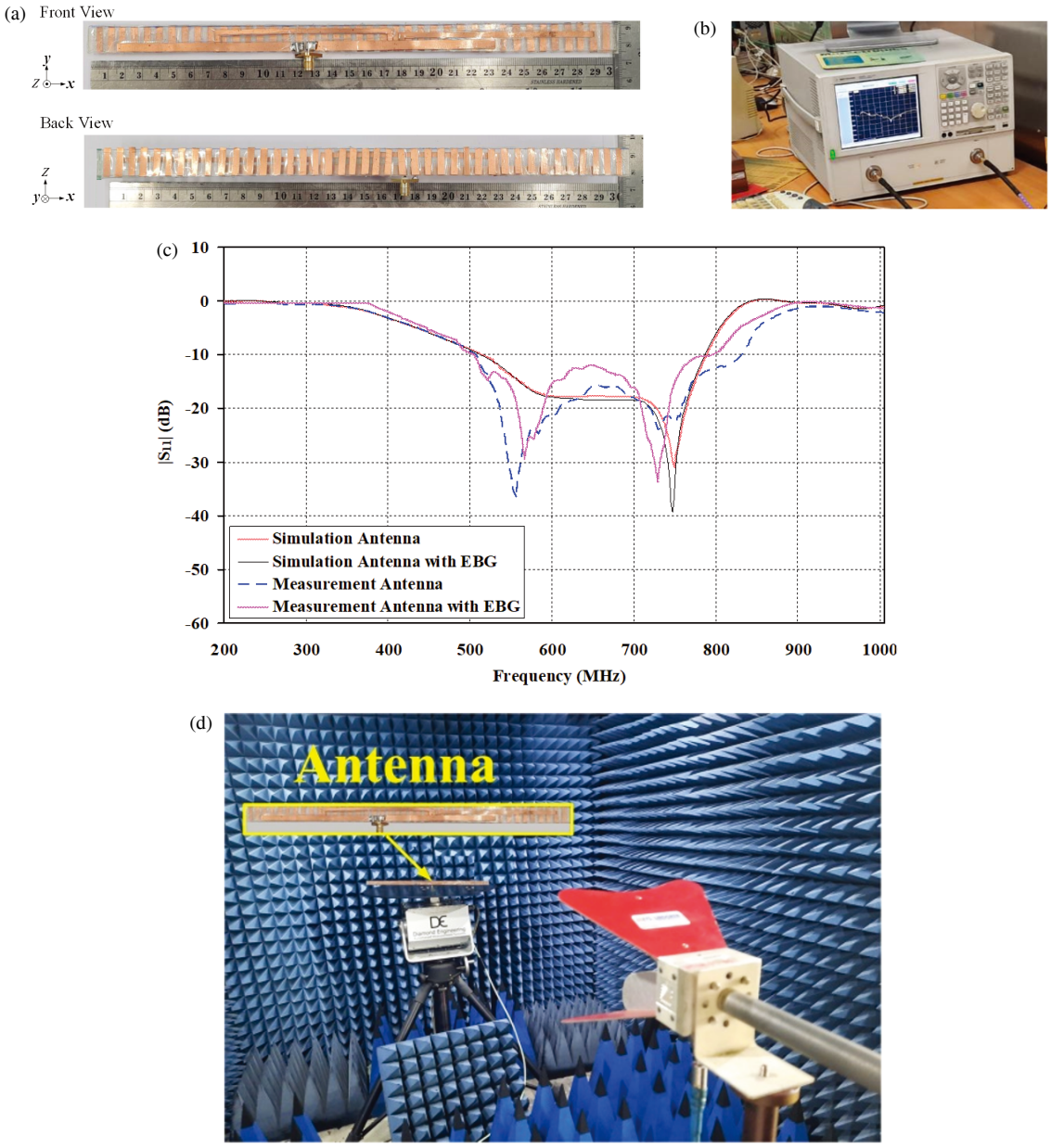

FIGURE 8. A prototype antenna (a) dipole antenna with I-shaped EBG (b) network analyzer (c) comparison results of simulation and measurement and (d) preparing antenna.

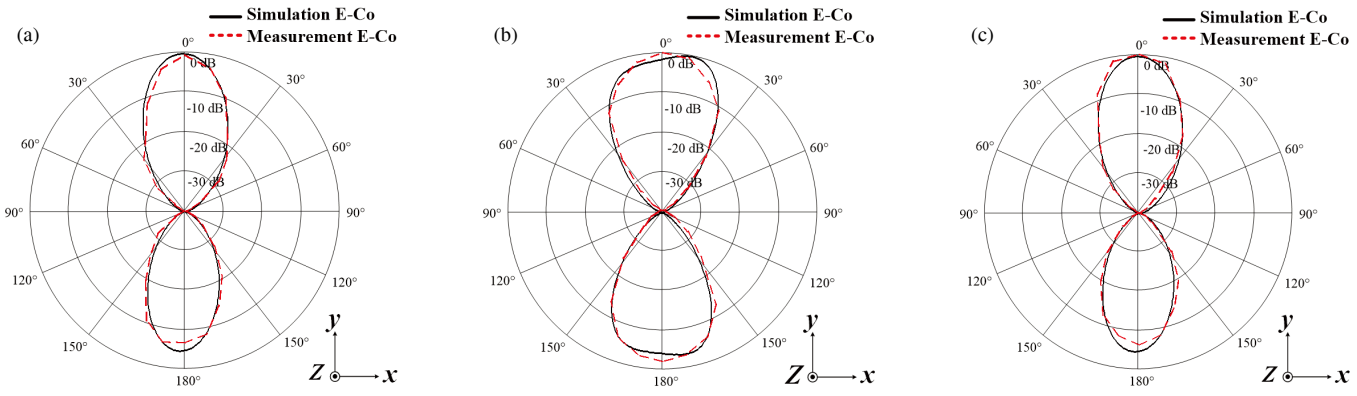

FIGURE 9. Comparison of radiation patterns in E-plane (a) at 510 MHz (b) at 650 MHz and (c) at 790 MHz.

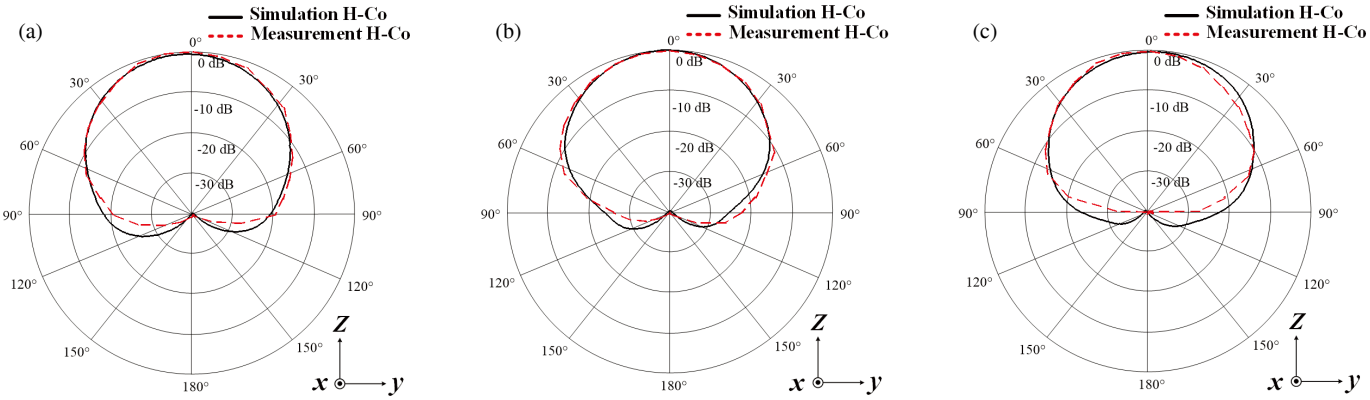

FIGURE 10. Comparison of radiation patterns in H-plane (a) at 510 MHz (b) at 650 MHz and (c) at 790 MHz.

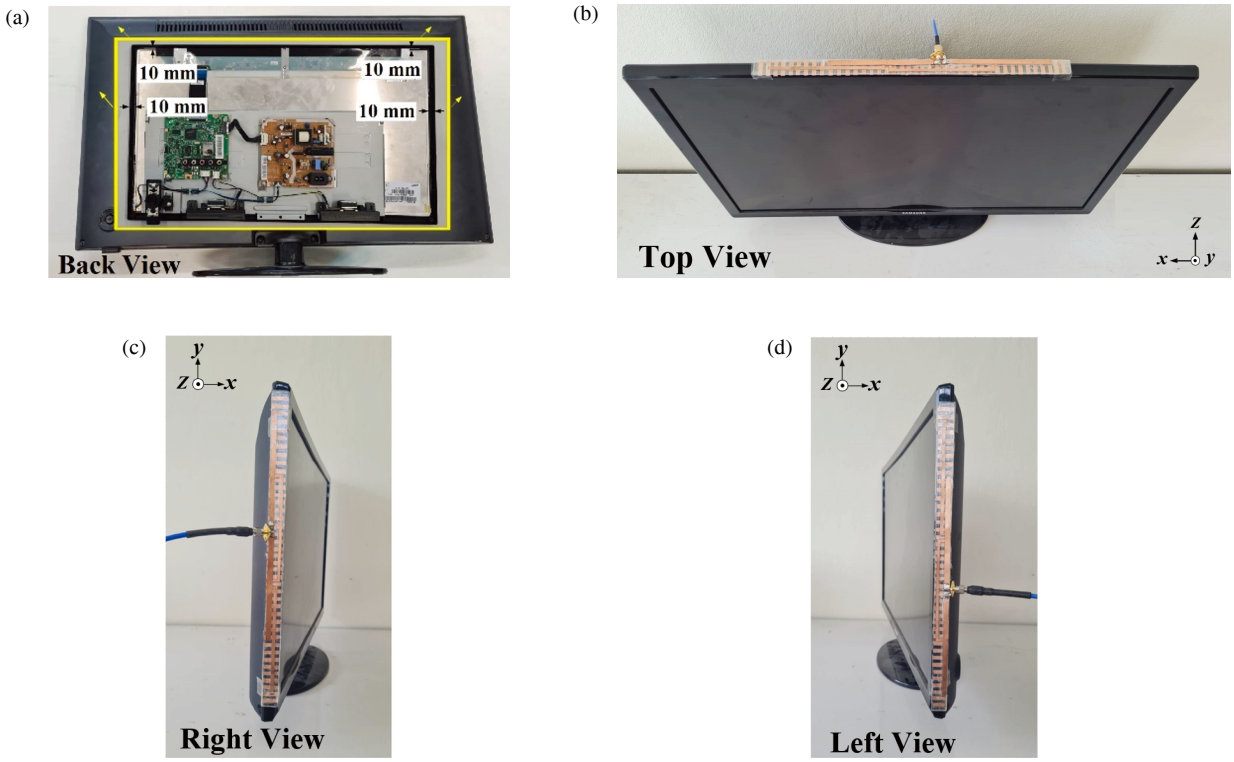

FIGURE 11. The experimental dipole antenna with digital TV (a) on top view (b) on right view and (c) on left view.

that the radiation patterns from the measurements and simulations tend to follow the same direction in both the E-plane and H-plane.

4. EXPERIMENTAL FOR PROTOTYPE ANTENNA WITH TELEVISION

In this section, we would test the placement of the prototype antenna on the television to evaluate the signal accuracy. We would use a Samsung TV model UA23F4003AR, with the screen positioned 10 mm away from the frame, as shown in Figure 11(a). The three configurations: top view, right view, and left view are shown in Figures 11(b)–(d), using the Lite VNA V2 Model 64 network analyzer as the signal transmitter. From the tests, it was found that placing the antenna on top resulted in the reflection coefficient ($S_{11} < -10$ dB) having the least effect on signal quality according to ATSC standards, which covers a frequency range of 44.32% (504–791 MHz). Since the circuit board and the built-in speakers in the television were spaced apart, the reflection of the waves did not transmit to the antenna, which had an effect similar to a dipole antenna with an EBG plate as desired. The other two sides that did not cover the frequency range were the right view, which had a frequency range of 34.42% (505–715 MHz) due to the reflection of waves from the circuits and speakers within the television, and the left view, which had a frequency range of 31.85% (504–695 MHz)

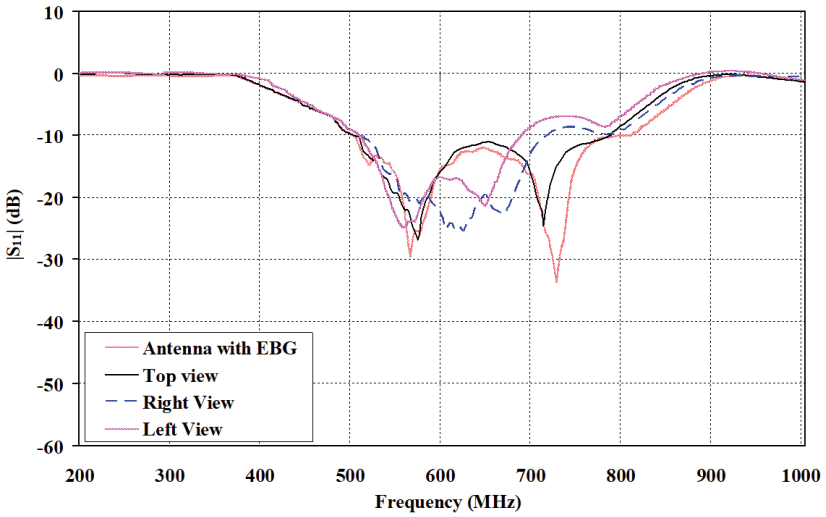

FIGURE 12. Measurement results of S_{11} of dipole antenna with digital TV.

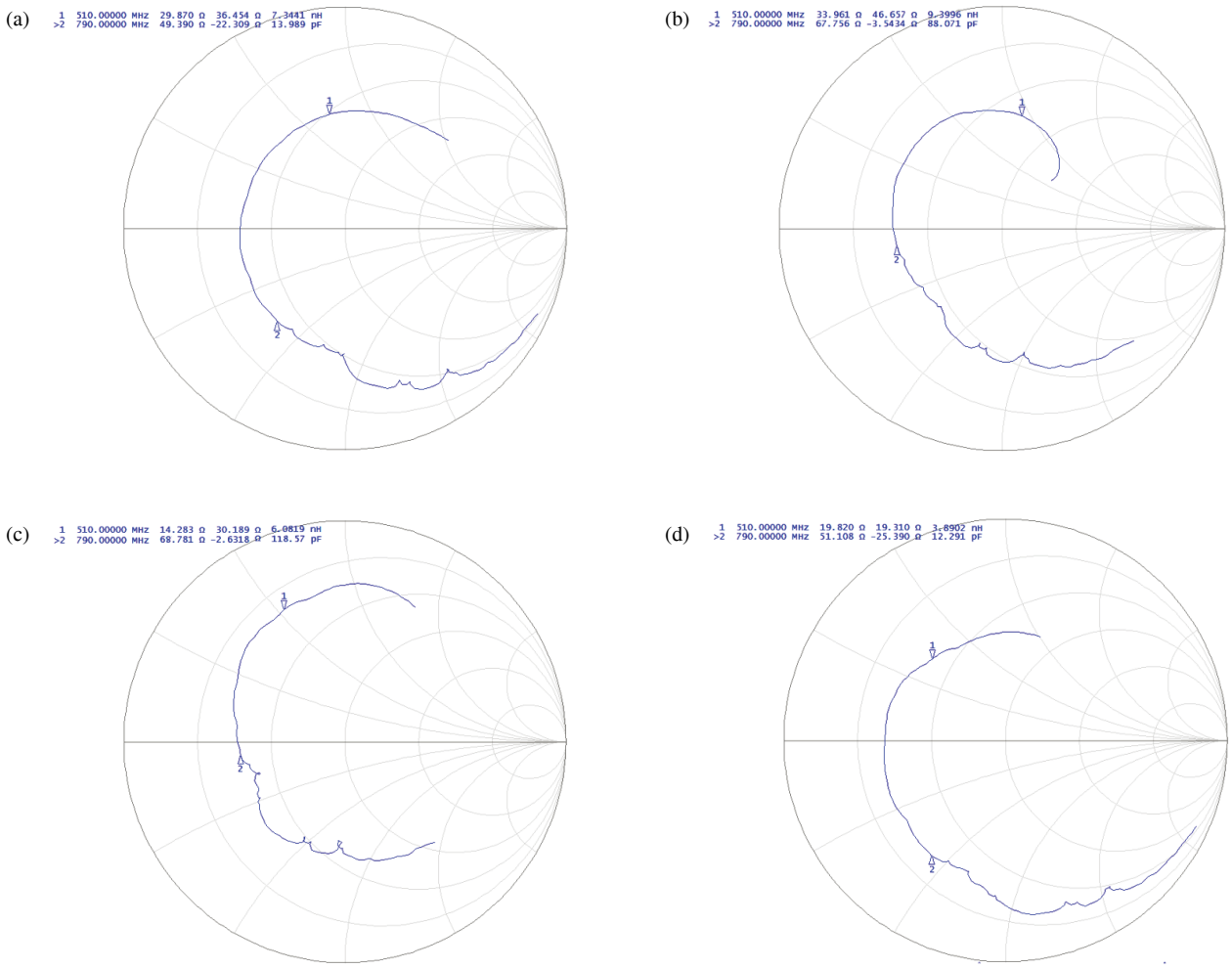

FIGURE 13. Comparison results of Smith chart plots of dipole antenna (a) antenna with EBG (b) top view (c) right view and (d) left view.

due to the reflection of waves from the circuits and speakers within the television that was closer than the right view, resulting in a smaller coverage of the frequency range, as shown in Figures 12–13 [36]. The results were shown the clearest in Table 3, and the gain from the simulation had an average of 3.65 dBi, while the measured result had an average of 3.62 dBi, which tends to be in the same direction as shown in Figure 14.

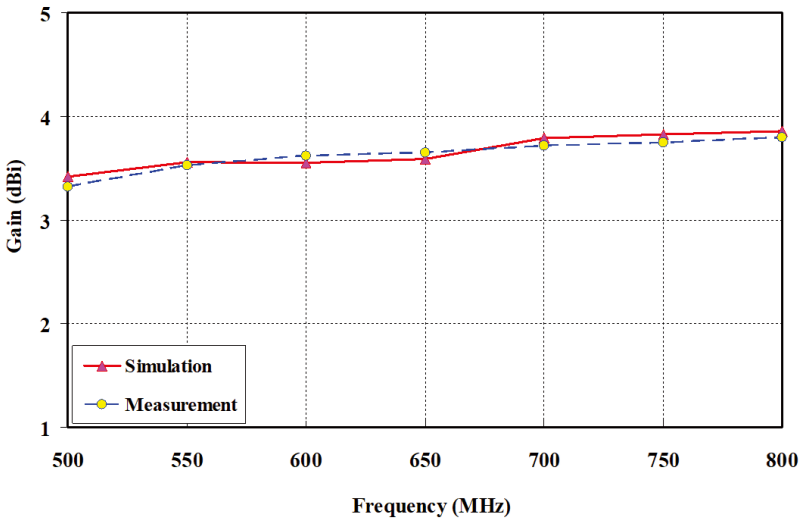

FIGURE 14. Comparison results of gains of simulation and measurement.

TABLE 3. Comparison of measurement results of dipole antenna with digital TV.

Antenna	BW (%)
Dipole with U-shape and L-shape and with EBG	46.01% (502–802 MHz)
Dipole with U-shape and L-shape and with EBG on top view of television	44.32% (504–791 MHz)
Dipole with U-shape and L-shape and with EBG on right view of television	34.42% (505–715 MHz)
Dipole with U-shape and L-shape and with EBG on left view of television	31.85% (504–695 MHz)

TABLE 4. Comparison of properties of all antenna.

Reference	Frequency (GHz)	Substrate	EBG Shaped	Size EBG (mm^3)	EBG (units)	Distance (mm)	Average Gain (dBi)
[9]	0.47–0.96	PET	Rectangular	100×320	3×11	4	5
[12]	0.92	FR4	H and I-shaped	326×0.5	$4 \times 1, 1 \times 5$	2	1.23
[15]	0.85–0.95	FR4	Square	$434 \times 434 \times 1.6$	7×7	4.8	5
[18]	0.876–992	FR4	Square	$800 \times 320 \times 2.6$	2×10	1.6	1.79
[23]	4.48–7.12	FR4	Square	$52.5 \times 52.5 \times 3$	5×5	3	8.4
[24]	24.7–29.9	FR4	Solder ball	$1.6 \times 1.6 \times 0.2$	14×12	1.4	9.5
[26]	2.42–2.7	Cloth	I-shaped	$48.32 \times 24.92 \times 3.2$	11×3	3.2	-
[27]	0.1–0.6	Fiberglass cloth	Rectangular	$1600 \times 100 \times 0.04$	1×1	40	3.8
[30]	0.47–0.862	FR4	Square	396×396	3×3	130	15
Proposed	0.504–0.791	Polyester mylar	I-shaped	$270 \times 15.5 \times 0.59$	1×41	2	3.62

5. COMPARATIVE ANALYSIS

The design of the dipole antenna structure was tuned with U-shaped and L-shaped stubs, along with 1×41 EGB, to support DVB operation in the frequency range of 510–790 MHz. The design used the adding stub technique which had less complex tuning than the research in [12, 18, 23, 24, 26, 27, 30], and the EBG plate in I-shaped was easily designed with a thin structure and a distance from the antenna of only 2 mm, which was less than the research in [9, 12, 15, 23, 26, 27, 30]. On the other hand, the research in [18, 24] had a distance of 1.6 mm and 1.4 mm, respectively, which was narrower than the presented research due to the thickness of the FR4 substrate. In the research presented in [9, 30], there was a frequency range used in the DVB band, but the shape of the antenna did not conform to the structure of the television as in the presented research. An overview comparing the various properties of all antennas with the presented antenna is shown in Table 4.

6. CONCLUSION

This research designs a dipole antenna using the technique of adding a U-shaped stub to increase the impedance bandwidth

in the high-frequency range and an L-shaped stub to increase the impedance bandwidth in the low-frequency range. The addition of both shapes of stubs results in the impedance bandwidth covering the entire operating frequency range of 44.37% (505–793 MHz), which complies with the ATSC standard for installation on televisions, using the technique of reducing reflection with I-shaped EBG, 1×41 units. The antenna was designed with a copper plate, using a polyester film as the substrate and foam as the intermediate material between the antenna and EBG plate. It was simulated using CST program to find the most suitable parameters, with an overall structure size of $270 \times 15.5 \times 0.59\,\text{mm}^3$. Then, a prototype antenna was fabricated. The measurement results showed that the impedance bandwidth trend was consistent with the simulation, with a unidirectional pattern across the frequency range and the antenna gain that also matched the simulation. When the antenna, placed 2 mm away from the EBG plate, was tested by installing it on top of the Samsung television model UA23F4003AR, the impedance bandwidth was measured to be 44.32% (504–791 MHz). It has an average gain of 3.62 dBi. The advantages of this antenna are its slim and lightweight design, simple and uncomplicated structure, and its ability to cover the frequency range used for digital TV in Thailand. It can be placed on TVs with thin metal edges that reflect signals, and it is compatible with all models and brands of TVs sold in Thailand.

The new antenna structure and EBG plate are designed to be simple and straightforward. The antenna and EBG plate can be effectively integrated, with the antenna positioned very close to the EBG plate. This minimal spacing is also maintained when the antenna is placed on the TV screen. In the next research, the antenna will be tested with other brands of televisions to develop the antenna to be compatible with all models of televisions in the future.

ACKNOWLEDGEMENT

The authors would like to thank Department of Aircraft Maintenance Engineering, Faculty of Railway Systems and Transportation for supporting the equipment assistance, Department of Telecommunication Engineering and Digital Innovation, Faculty of Engineering and Technology for CST Studio Suite electromagnetic simulation software, Rajamangala University of Technology Isan, Department of Electrical Engineering, Faculty of Engineering and Architecture, Rajamangala University of Technology Suvarnabhumi, and Department of Mechatronics and Robotics Engineering, School of Engineering and Innovation, Rajamangala University of Technology Tawan-ok for the sample of raw materials and equipment.

REFERENCES

[1] Song, J., Z. Yang, and J. Wang, *Digital Terrestrial Television Broadcasting: Technology and System*, John Wiley & Sons, 2015.

[2] Komsing, S., N. Fhafhiem, A. Innok, and A. Ruengwaree, "Design of wide-band dipole antenna for digital TV broadcasting application," in *2018 International Electrical Engineering Congress (iEECON)*, 1–4, Krabi, Thailand, 2018.

[3] Van Trinh, T., B. Lee, T. Park, and C. W. Jung, "Internal reconfigurable dipole–loop antenna array for high reception rate of wideband UHD-TV applications," *Journal of Electrical Engineering & Technology*, Vol. 14, 2427–2436, 2019.

[4] Duangtang, P. and R. Wongsan, "Design of band-notched planar dipole antenna for DTV application," in *2019 7th International Electrical Engineering Congress (iEECON)*, 1–4, Hua Hin, Thailand, 2019.

[5] Kampeephat, S., S. Todsungnoen, P. Kamphikul, and W. Sarikha, "A study of impedance bandwidth improvement of printed dipole antenna for DTV," in *2021 18th International Conference on Electrical Engineering/Electronics, Computer, Telecommunications and Information Technology (ECTI-CON)*, 341–344, Chiang Mai, Thailand, 2021.

[6] Sanad, M. and N. Hassan, "An internal EBG antenna for indoor reception of UHF terrestrial digital TV broadcasting," in *2010 10th Mediterranean Microwave Symposium*, 178–181, Guzelyurt, Northern Cyprus, 2010.

[7] Lee, Y., A. Goudelev, B. Kim, and W. Hong, "Metal chassis robust antenna on compact AMC structure for commercial slim TV," in *2014 IEEE Antennas and Propagation Society International Symposium (APSURSI)*, 396–397, Memphis, TN, USA, 2014.

[8] Chou, H.-T. and H.-J. Su, "Dual-band hybrid antenna structure with spatial diversity for DTV and WLAN applications," *IEEE Transactions on Antennas and Propagation*, Vol. 65, No. 9, 4850–4853, 2017.

[9] Sanad, M. and N. Hassan, "A novel internal dual-polarized EBG antenna for indoor reception of UHF terrestrial digital TV broadcasting," *International Journal of Microwave Science and Technology*, Vol. 2012, No. 1, 873126, 2012.

[10] Elwi, T. A., "A slotted lotus-shaped microstrip antenna based EBG structures," *Wireless Communication Technology*, Vol. 2, No. 1, 1–24, 2018.

[11] Guo, W., M.-C. Tang, Y. Wang, and M. Li, "Wideband, electrically small filtenna based on electromagnetic band-gap structure," in *2019 Cross Strait Quad-Regional Radio Science and Wireless Technology Conference (CSQRWC)*, 1–3, Taiyuan, China, 2019.

[12] Kwon, J., H. Park, C. Lee, G. Namgung, Y. Seo, S. Kahng, and J. Kim, "A compact EBG for high isolation between two very closeby wire-antennas for RFID tags," in *2019 IEEE International Symposium on Antennas and Propagation and USNC-URSI Radio Science Meeting*, 1189–1190, Atlanta, GA, USA, 2019.

[13] Yalduz, H., B. Koç, L. Kuzu, and M. Turkmen, "An ultra-wide band low-SAR flexible metasurface-enabled antenna for WBAN applications," *Applied Physics A*, Vol. 125, No. 9, 609, 2019.

[14] Liu, D. Q., H. J. Luo, M. Zhang, H. L. Wen, B. Wang, and J. Wang, "An extremely low-profile wideband MIMO antenna for 5G smartphones," *IEEE Transactions on Antennas and Propagation*, Vol. 67, No. 9, 5772–5780, 2019.

[15] Gupta, G. and A. R. Harish, "Feeds for dipole over high impedance surface," in *2019 IEEE Indian Conference on Antennas and Propogation (InCAP)*, 1–4, Ahmedabad, India, 2019.

[16] Liu, F., J. Guo, L. Zhao, G.-L. Huang, Y. Li, and Y. Yin, "Dual-band metasurface-based decoupling method for two closely packed dual-band antennas," *IEEE Transactions on Antennas and Propagation*, Vol. 68, No. 1, 552–557, 2020.

[17] Arif, A., M. R. Akram, K. Riaz, M. Zubair, and M. Q. Mehmood, "Koch fractal based wearable antenna backed with EBG plane," in *2020 17th International Bhurban Conference on Applied Sciences and Technology (IBCAST)*, 642–646, Islamabad, Pakistan,

2020.

[18] Li, X., G. Gao, H. Zhu, Q. Li, N. Zhang, and Z. Qi, "UHF RFID tag antenna based on the DLS-EBG structure for metallic objects," *IET Microwaves, Antennas & Propagation*, Vol. 14, No. 7, 567–572, 2020.

[19] Subramanian, S., P. M. Parameswari, and B. Sundarambal, "Design and development of RF energy harvesting loop antenna," in *2020 6th International Conference on Advanced Computing and Communication Systems (ICACCS)*, 994–997, Coimbatore, India, Mar. 2020.

[20] Qureshi, S. A., A. Y. I. Ashyap, Z. Z. Abidin, S. H. Dahlan, S. M. Shah, S. K. Yee, H. A. Majid, and C. H. See, "Compact, low-profile and robust inversely E-shaped antenna integrated with EBG structures for wearable application," in *2020 IEEE Student Conference on Research and Development (SCOReD)*, 28–32, Batu Pahat, Malaysia, 2020.

[21] Bora, P., P. Pardhasaradhi, and B. T. P. Madhav, "Design and analysis of EBG antenna for Wi-Fi, LTE, and WLAN applications," *Applied Computational Electromagnetics Society Journal (ACES)*, Vol. 35, No. 9, 1030–1036, 2020.

[22] Da, Y., T. Li, Q. Li, X. Chen, and A. Zhang, "A dual-polarized antenna array for base station applications," in *2020 IEEE 3rd International Conference on Electronic Information and Communication Technology (ICEICT)*, 590–593, Shenzhen, China, 2020.

[23] Malekpoor, H. and M. Hamidkhani, "Performance enhancement of low-profile wideband multi-element MIMO arrays backed by AMC surface for vehicular wireless communications," *IEEE Access*, Vol. 9, 166 206–166 222, 2021.

[24] Liu, X., W. Zhang, D. Hao, and Y. Liu, "Broadband surface-mount dipole antenna array using highly isolated via fence for 5G millimeter-wave applications," *Progress In Electromagnetics Research Letters*, Vol. 100, 27–34, 2021.

[25] Ramanpreet, N., M. Rattan, and S. S. Gill, "Compact and low profile planar antenna with novel metastructure for wearable MBAN devices," *Wireless Personal Communications*, Vol. 118, 3335–3347, 2021.

[26] El-Bacha, M., F. Ferrero, and L. Lizzi, "Wearable waveguide surface for low-loss body area network communications," *IEEE Antennas and Wireless Propagation Letters*, Vol. 20, No. 12, 2295–2299, 2021.

[27] Chen, X., H. Wu, and G. Fu, "Wideband VHF/UHF wing conformal vertical polarized omnidirectional antenna," *IEEE Antennas and Wireless Propagation Letters*, Vol. 21, No. 5, 953–957, 2022.

[28] Ashyap, A. Y. I., S. H. B. Dahlan, Z. Z. Abidin, M. I. Abbasi, M. R. Kamarudin, H. A. Majid, M. H. Dahri, M. H. Jamaluddin, and A. Alomainy, "An overview of electromagnetic band-gap integrated wearable antennas," *IEEE Access*, Vol. 8, 7641–7658, 2020.

[29] Zheng, Q., C. Guo, G. A. E. Vandenbosch, and J. Ding, "Low-profile circularly polarized array with gain enhancement and RCS reduction using polarization conversion EBG structures," *IEEE Transactions on Antennas and Propagation*, Vol. 68, No. 3, 2440–2445, Mar. 2020.

[30] Pimpol, S. and R. Wongsan, "Wide-bandwidth and flat-gain printed dipole with EBG reflector for terrestrial DTV reception," *Suranaree Journal of Science & Technology*, Vol. 24, No. 2, 179–192, 2017.

[31] Sara, S. and E.-S. Abdenacer, "Novel dual-band dipole antenna integrated with EBG electromagnetic bandgap structures dedicated to mobile communications," in *2019 International Conference on Wireless Technologies, Embedded and Intelligent Systems (WITS)*, 1–5, Fez, Morocco, Apr. 2019.

[32] Chen, D., W. Yang, W. Che, Q. Xue, and L. Gu, "Polarization-reconfigurable and frequency-tunable dipole antenna using active AMC structures," *IEEE Access*, Vol. 7, 77 792–77 803, 2019.

[33] Naktong, W., A. Ruengwaree, N. Fhafhiem, and P. Krachodnok, "Resonator rectenna design based on metamaterials for low-RF energy harvesting," *Computers, Materials & Continua*, Vol. 68, No. 2, 1731–1750, 2021.

[34] Yang, F., S. Xu, and Y. Rahmat-Samii, "Surface electromagnetics: Historic development and antenna applications," in *2019 URSI International Symposium on Electromagnetic Theory (EMTS)*, 1–3, San Diego, CA, USA, 2019.

[35] Balanis, C. A., *Antenna Theory: Analysis and Design*, John Wiley & Sons, 2016.

[36] Mukherjee, B., P. Patel, and J. Mukherjee, "Hemispherical dielectric resonator antenna based on apollonian gasket of circles — A fractal approach," *IEEE Transactions on Antennas and Propagation*, Vol. 62, No. 1, 40–47, 2013.